Multiscale Mechanical Evaluation of Human Supraspinatus Tendon Under Shear Loading After Glycosaminoglycan Reduction

Fei Fang
Department of Mechanical Engineering
and Materials Science,
Washington University in St. Louis,
1 Brookings Drive,
Campus Box 1185,
St. Louis, MO 63130
e-mail: fangfei@wustl.edu

Spencer P. Lake[1]
Department of Mechanical Engineering
and Materials Science,
Washington University in St. Louis,
1 Brookings Drive,
Campus Box 1185,
St. Louis, MO 63130;
Department of Biomedical Engineering,
Washington University in St. Louis,
1 Brookings Drive,
Campus Box 1185,
St. Louis, MO 63130;
Department of Orthopaedic Surgery,
Washington University in St. Louis,
1 Brookings Drive,
Campus Box 1185,
St. Louis, MO 63130
e-mail: lake.s@wustl.edu

Proteoglycans (PGs) are broadly distributed within many soft tissues and, among other roles, often contribute to mechanical properties. Although PGs, consisting of a core protein and glycosaminoglycan (GAG) sidechains, were once hypothesized to regulate stress/strain transfer between collagen fibrils and help support load in tendon, several studies have reported no changes to tensile mechanics after GAG depletion. Since GAGs are known to help sustain nontensile loading in other tissues, we hypothesized that GAGs might help support shear loading in human supraspinatus tendon (SST), a commonly injured tendon which functions in a complex multiaxial loading environment. Therefore, the objective of this study was to determine whether GAGs contribute to the response of SST to shear, specifically in terms of multiscale mechanical properties and mechanisms of microscale matrix deformation. Results showed that chondroitinase ABC (ChABC) treatment digested GAGs in SST while not disrupting collagen fibers. Peak and equilibrium shear stresses decreased only slightly after ChABC treatment and were not significantly different from pretreatment values. Reduced stress ratios were computed and shown to be slightly greater after ChABC treatment compared to phosphate-buffered saline (PBS) incubation without enzyme, suggesting that these relatively small changes in stress values were not due strictly to tissue swelling. Microscale deformations were also not different after ChABC treatment. This study demonstrates that GAGs possibly play a minor role in contributing to the mechanical behavior of SST in shear, but are not a key tissue constituent to regulate shear mechanics. [DOI: 10.1115/1.4036602]

Keywords: glycosaminoglycans, supraspinatus tendon, shear, mechanical properties, enzyme treatment

1 Introduction

Injury, disease, and age-related degeneration of tendon often lead to deteriorated mechanical properties and loss of function [1]. To address the origins of altered mechanical behavior, the structural and compositional properties of tendons in heathy or diseased states have been characterized to elucidate how these factors contribute to mechanical function [2,3]. In addition, treatment strategies for tendon injuries seek to promote the formation of normal structural and compositional properties in order to restore a suitable environment to promote cell-mediated tissue remodeling and sustain in vivo mechanical loading. Therefore, tendon structure and function not only dictate mechanical properties, but also are key indicators to help evaluate treatment efficiency.

Previous literature has established that tendon is mainly composed of collagen type I, with minor amounts of other extracellular matrix (ECM) components, including other types of collagen, glycoproteins, elastin, and PGs [3]. Although collagen type I is the principal tendon component that supports mechanical loading, other constituents, especially elastin and PGs, have been suggested to contribute to tendon mechanics [4,5]. PGs, consisting of a core protein with attached GAG sidechains, are observed in the interfascicular matrix of tendons and in specific regions of some tendons (i.e., flexor tendon, supraspinatus tendon) that experience multiaxial loading [6,7]. Besides being present in healthy tendon, increased GAGs have been shown to collocate with disorganized collagen fibers, and expression of PGs (e.g., aggrecan and biglycan) is prominently upregulated in injured tendons [8,9]. Therefore, evaluation of PG/GAG quantity and distribution has been regarded as an essential task to address tendon structure–function relationships [10,11].

Knockout animal models and degradation via enzyme treatment have been adopted as two common approaches to examine the role of PGs and GAG side chains in tendon function from both biochemical and mechanical perspectives [9,12–17]. Using such techniques, small leucine-rich PGs (i.e., decorin, biglycan) have been shown to modulate the functional activity of growth factors and cell surface receptors and provide regulatory effects (e.g., collagen fibrillogenesis) in tendon that often have mechanical implications [15,16,18]. Another study suggested that decorin and biglycan bind calcium ions and promote mineralization of tendon collagen fibrils [19]. Regarding direct mechanical contributions, PGs undoubtedly help sustain compressive loading in tendon (e.g., through water bound to the GAG sidechains of the large PG aggrecan) [20,21], similar to their demonstrated role in cartilage [22–25]. However, tensile testing of enzymatically treated tendon/ligament showed that GAG degradation did not alter mechanical

[1]Corresponding author.

Manuscript received November 30, 2016; final manuscript received April 26, 2017; published online June 6, 2017. Assoc. Editor: Eric A Kennedy.

parameters, suggesting that GAGs do not contribute directly to tensile mechanics of tendon/ligament [26–28]. These results contradict a previously proposed theoretical mechanism, wherein PG core proteins bind to collagen fibrils, and GAGs cross-link fibrils to increase tensile strength of connective tissues [29], as well as the previous results showing that GAGs contribute to the mechanics of other soft tissues such as arterial wall and sclera [30,31].

Determining whether GAGs play a role in tendon mechanical properties under other nontensile loading conditions (i.e., shear, torsion) represents an important additional approach to fully consider their potential contribution to tendon function. One previous study of human medial collateral ligament showed unaltered shear stresses before and after GAG digestion via chondroitinase B treatment [28]. Still, it remains unclear whether GAGs play a mechanical role at both macro- and microscales in tendons that experience significant nontensile loading during normal physiological function. Human SST, the most commonly injured tendon of the rotator cuff in the shoulder [32], is subjected to complex multiaxial loading (i.e., tension, shear, compression) in vivo, including intratendinous shear strain through the tendon thickness during glenohumeral abduction [33]. The complex mechanical nature of the physiological SST environment likely contributes to the unique region-specific tensile mechanical properties, collagen organization, and PG distribution of this tissue [33–35]. While our previous work showed that elastin depletion altered shear mechanics of SST, [9] it is unknown if PGs and corresponding GAG sidechains also facilitate the mechanical response of SST to shear loading. Moreover, even with only moderate/minor changes in macroscale shear mechanics following GAG depletion, microscale deformations of treated tendons could potentially exhibit differences due to disrupted microstructural integrity of collagenous matrix and adjacent GAGs. Therefore, using a multiscale experimental approach to simultaneously evaluate macroscale mechanical properties and microscale deformation of SSTs with intact or digested GAGs can help address mechanisms governing the behavior/role of GAGs in the shear behavior of tendons which experience significant nontensile physiologic loads.

The goal of this study was to quantify multiscale mechanical behavior of human SST before and after removing GAGs to understand how GAGs contribute to shear response of this complex and unique tendon. Biomechanical shear test through tendon thickness was performed on samples from specific regions of human SST with microscale deformation modes simultaneously recorded via two-photon microscopy. Based on the previous proposition that GAGs might bridge adjacent collagen fibrils and consequently help stress transfer to the higher-scale fibers, and that SSTs are suggested to have greater amounts of GAG content compared to other connective tissues, we hypothesized that GAG depletion in SST would lead to inferior mechanical properties on the macro- and microscales, including decreased peak/equilibrium stresses and increased local-matrix-based measures of deformation (i.e., strain and rotation).

2 Materials and Methods

2.1 Chondroitinase ABC Treatment Protocol. A series of concentration- and time-dependent tests were conducted to determine an appropriate treatment protocol using chondroitinase ABC (ChABC), which can degrade GAG chains from tendon. The medial region of a single SST was used to obtain small tissue specimens ($n = 15$) with approximate dimensions of $1 \times 0.5 \times 0.5$ mm^3 and weights of 40–50 mg. To optimize enzyme concentration, specimens were randomly assigned to be incubated in 30 ml pH = 8 buffer containing 50 mM Tris, 60 mM sodium acetate, 0.02% bovine serum albumin with 0 (control), 0.1, 0.2, 0.3, and 0.4 units/ml ChABC ($n = 3$ for each concentration, C2905, Sigma-Aldrich, St. Louis, MO) for 6 h at room temperature [9]. To optimize enzyme incubation time, similar specimens ($n = 15$) were harvested and incubated in 30 ml buffer with 0.2 units/ml ChABC for 0 (control), 1, 3, 8, 16 h at room temperature. After ChABC treatment, a dimethylmethylene blue (DMMB) colorimetric assay was used to quantify GAG content, reflecting PG amount, in all specimens [12,13,29]. After tissue digestion via papain (papain from papaya latex, P4762, Sigma-Aldrich, St. Louis, MO), 1-9-dimethylmethylene blue (DMMB, 341088, Sigma_Aldrich, St. Louis, MO) was added to the tissue solution in standard 96-well plates. Intensity of 595 nm wavelength light was quantified for each sample by spectrometry and compared to standard curve data to determine GAG content, which was normalized by sample wet weight [36].

Since the attachment of relatively large mechanically tested samples to shear clamps partially blocks enzymatic solution from contacting sample surfaces during incubation, the penetration of ChABC into full-size clamped samples was also evaluated. Human SST exhibits heterogeneous collagen organization and GAG distribution, making it challenging to evaluate penetration of enzymatic degradation [5]. Our preliminary data found that bovine deep digital flexor tendon (DDFT) had a constant distribution of GAGs ($0.21 \pm 0.02\%$ normalized by wet weight) in the proximal region, consistent with previous studies [7,37]. Therefore, the proximal region of DDFT was used as a representative model for this quantification. Two adjacent and paired samples ($n = 4$) with the same size as mechanically tested samples were harvested from the proximal region of four bovine DDFTs, as done previously [6,7,38]. Samples were glued to shear test clamps; one clamps-sample assembly was incubated in PBS for 8 h as the control, and the other incubated in 0.2 units/ml ChABC buffer for 8 h. After incubation, thin pieces of specimens weighing 40–50 mg were carefully collected at five locations evenly spaced along the treating buffer depth from treated/incubated samples for biochemical analysis. The normalized sample width (marked by the arrow inside the block, Fig. 1(*c*)) was taken as 1, and the sample surface was defined as 0. Normalized GAG content was computed as the ratio of GAGs in treated samples relative to corresponding controls along the sample width.

2.2 Biomechanical Tests. Using results from our previous multiscale studies of bovine flexor tendon [6,7], a power analysis (power = 0.8; $\alpha = 0.05$) determined that a sample size of $n = 7$ would be sufficient to find differences in stress and microscale strain values of at least 4 kPa and 4%, respectively, before and after enzyme depletion. Seven cadaveric shoulder specimens (mean age: 61.3 ± 14.6 yr) with no evidence of tendon damage were dissected to harvest SSTs. As described in the previous studies [9,34,35], full-thickness samples were obtained from anterior, posterior, and medial regions of SST for biomechanical tests, and an adjacent specimen was harvested from each sample as control tissue for biochemical or histological analysis. After the surfaces of mechanically tested samples were leveled on a freezing-stage microtome, cross-sectional area and thickness were measured by a noncontact laser scanning system (Keyence, Elmwood Park, NJ) [9].

Samples, stained with 5-dichlorotriazinyl aminofluorescein and diamidino phenylindole to visualize collagen and nuclei as done previously [6,9], were mounted in a biomechanical test device combined with a Zeiss two-photon confocal microscope [6,9]. The test system, applied shear loading protocol, and image acquisition settings/timings were adopted from the previous studies [9], which compared the mechanical response of human SST in shear after elastase treatment. Accordingly, after preloading samples, photobleached grids were created with four adjacent $100 \times 100\ \mu$m squares at a depth of $50\ \mu$m at each of the three locations evenly spaced along the sample thickness (Fig. 2). Step-increases of 0.08, 0.16, and 0.24 shear strains with 12-min relaxation periods between each strain value were incrementally applied. Multichannel z-stacks of photobleached squares were collected after preload and 8 min after each incrementally applied strain [6,9]. Following the test protocol, samples were kept

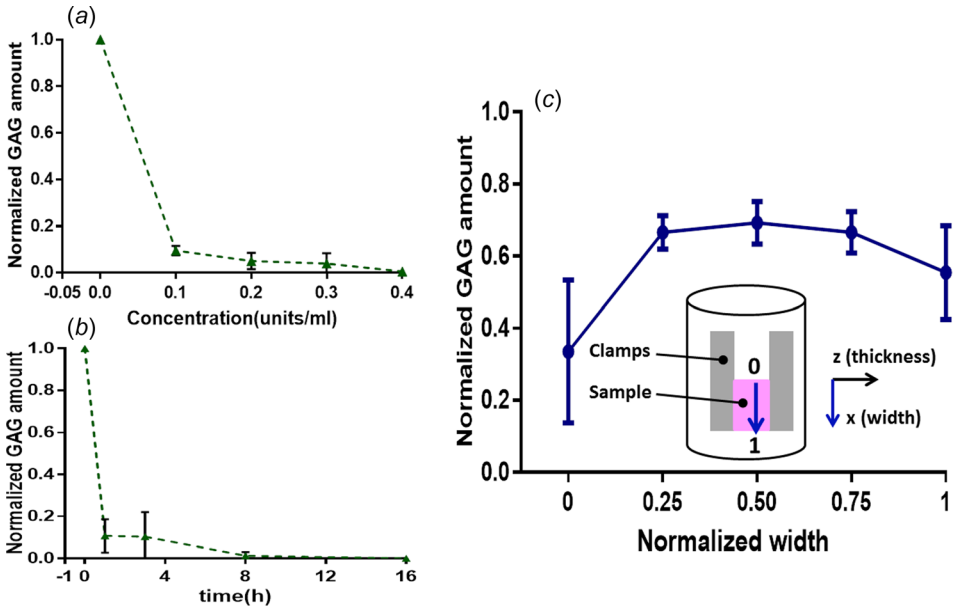

Fig. 1 Normalized GAG amounts in SST samples treated for 6 h with different concentrations of ChABC buffer (*a*) or with 0.2 units/ml ChABC buffer for different durations of incubation (*b*). (*c*) GAG amount within DDFT after ChABC treatment exhibited a gradient distribution along the sample width; inset displays how clamps (left and right blocks) and attached sample (middle block) are secured for incubation and the subsequent mechanical test, where the normalized width is shown as 0 (top) to 1 (bottom) and is indicated as the *x* axis in the plot.

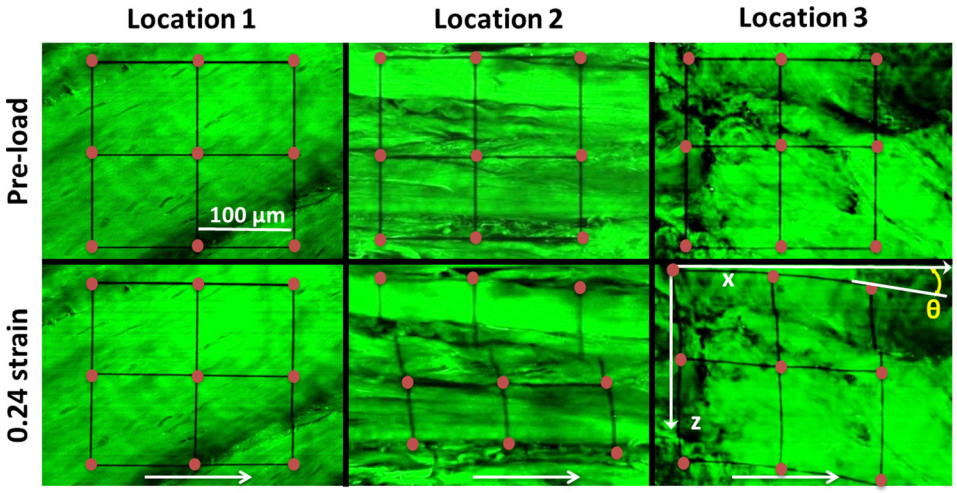

Fig. 2 Microscopy images from three locations of the same sample before and after application of 0.24 shear strain. Different locations within one sample from a single SST region showed heterogeneous organization of collagen fibers and different modes of deformation: no obvious deformation at location 1; fiber sliding at location 2; fiber reorganization at location 3. Rotation angle, θ, was calculated as the angle between the horizontal axis of images and deformed photobleached grids. Grid intersection points (dots added for visualization purpose only) were used to calculate local-matrix-based strain, while white arrows show shear loading direction.

attached to clamps, and clamp-sample assemblies were treated with the previously optimized enzyme protocol (see Sec. 3.1), namely 0.2 units/ml ChABC buffer for 8 h. Following ChABC treatment, photobleached squares were recreated again on the same three sample locations (or on nearby locations if the previous photobleached grids were not sharp) for image analysis. The shear loading protocol and image acquisition were then performed again for all treated samples. Control data from our prior study [9], namely shear test data of SST samples before and after PBS incubation (without enzyme treatment), were employed here to compare the effects of PBS incubation and GAG depletion on SST mechanical properties.

2.3 Evaluation of Treatment Efficiency. After the completion of biomechanical tests, ten samples and corresponding controls were randomly selected for DMMB assay. Three tissue segments weighing 40–50 mg were collected from each sample

evenly along sample width to quantify GAG content, as discussed in Sec. 2.1.

The efficiency of ChABC treatment was also evaluated using histological analysis of mechanically tested samples and paired controls from three regions of each of two SSTs (i.e., anterior, posterior, medial). Samples were fixed in 4% paraformaldehyde for 24 h, dehydrated in 70% ethanol, and embedded in paraffin. Paraffin sections (5-μm thickness) were obtained from both the top surface and middle portion of mechanically tested samples. From location-matched control samples, histological sections were taken from the paired/mirrored surface that was opposite to the analyzed/imaged surface of mechanically tested samples. Sections were stained with hematoxylin and eosin (H&E) or Alcian blue and imaged via bright field microscopy with 10× and 40× objectives. Typical images representative of collagen organization and GAG distribution were selected for presentation.

2.4 Data Analysis. For biochemical data, GAG amounts from tendon specimens/samples after ChABC treatment were normalized by GAG content of corresponding (nonincubated) controls. Peak (σ_p) and equilibrium (σ_e) stresses were calculated as force values immediately after each strain step and each 12-min stress–relaxation period, respectively, divided by cross-sectional areas (dimensions in xy plane in Fig. 1(*c*)). Normalized stresses were computed by dividing stresses from the second shear tests of ChABC-treated samples by the peak stress value (at 0.24 strain) from the first shear test (i.e., before incubation) of the same sample. The relaxation percent, peak reduced ratio, and equilibrium reduced ratio were evaluated as follows:

$$\text{Relaxation percent}\ (\%) = 100\frac{\sigma_p - \sigma_e}{\sigma_p} \tag{1}$$

$$\text{Peak reduced ratio}\ (\%) = 100\frac{\sigma_{p2} - \sigma_{p1}}{\sigma_{p1}} \tag{2}$$

$$\text{Equilibrium reduced ratio}\ (\%) = 100\frac{\sigma_{e2} - \sigma_{e1}}{\sigma_{e1}} \tag{3}$$

where σ_{p2} and σ_{p1} are peak stresses for the first and second shear tests, and σ_{e2} and σ_{e1} are equilibrium stresses for the first and second shear tests.

As shown in our previous studies [6,9], local-matrix-based strains were calculated as 2D Lagrangian strains by tracking photobleached squares visualized in microscopic images. Rotations, which characterize rigid body motion of photobleached squares, were defined as the average angle between the image x-axis and deformed horizontal photobleached grids (Fig. 2).

PRISM software (GraphPad Software, Inc., La Jolla, CA) was used to perform statistical analysis. Differences in output parameters by SST regions (anterior, posterior, and medial) were evaluated by one-way analysis of variances (ANOVAs) and post hoc comparisons with Bonferroni corrections. Mechanical differences (i.e., peak stress, equilibrium stress, relaxation percent) before and after ChABC treatment were determined by paired t-tests. To evaluate local-matrix-based strains and rotations, unpaired t-tests were used; a few issues in acquiring image stacks for the same samples before and after treatment precluded paired analysis. Unpaired t-tests were also used to compare mechanical parameters (peak reduced ratio, equilibrium reduced ratio) for PBS- and ChABC-incubated samples. Statistical significance was set at $p < 0.05$.

3 Results

3.1 Quantification of Treatment Efficiency. Untreated human SSTs had 0.282 ± 0.0383% GAGs (percent of wet weight) and no significant differences of GAG content were found by SST region (anterior, posterior, and medial). For the small tissue specimens, all enzyme treatment protocols decreased GAG amount dramatically (Figs. 1(*a*) and 1(*b*)). In terms of increasing enzyme concentration, GAG content appeared to plateau (at ~5%

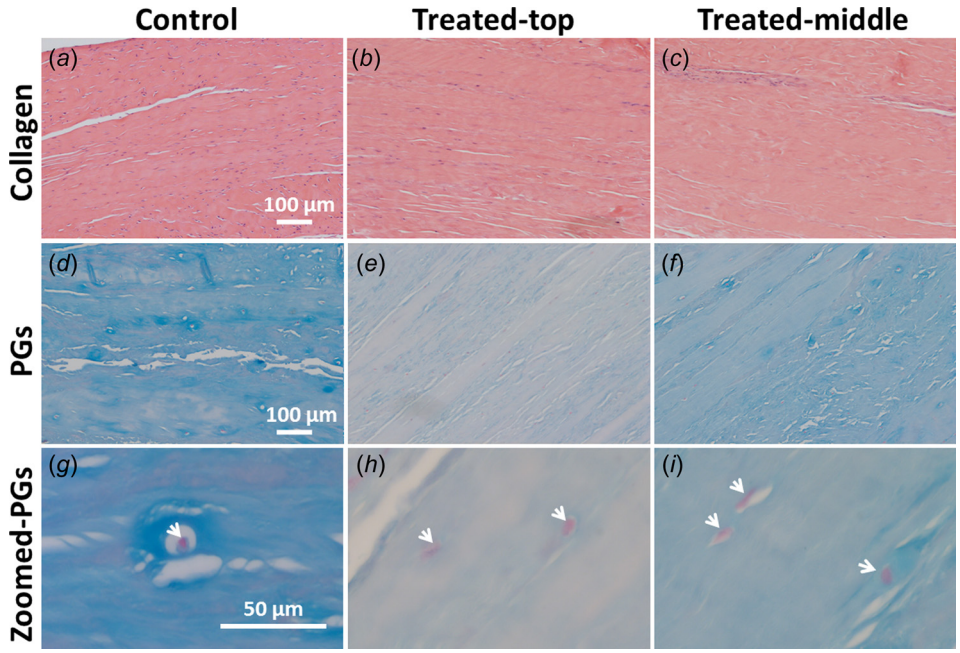

Fig. 3 Typical histological images of paired control and treated SST samples, which were stained by H&E and Alcian blue to show collagenous ECM ((*a*)–(*c*)) and GAGs ((*d*)–(*i*)), respectively. After ChABC treatment, the ECM was not visibly disrupted. GAG amount decreased differentially by location within each sample (demonstrated by varying intensity of staining in (*e*) and (*f*) compared to (*d*)), and GAG-rich pericellular matrix was observed to have been particularly degraded. Images (*a*)–(*f*) were acquired by 10× objective and images (*g*)–(*i*) by 40× objective. Treated-top and treated-middle are sections from the top and middle of treated samples, respectively. Arrows in images (*g*)–(*i*) denote cell nuclei.

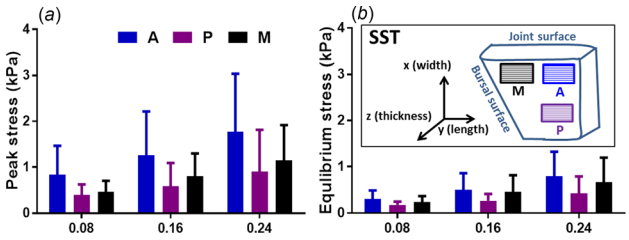

Fig. 4 Peak (*a*) and equilibrium (*b*) stresses for control (untreated) samples increased at larger strain steps, but were not significantly different across three SST regions; inset shows three regions (M = medial; A = anterior; P = posterior) in SSTs (mean ± SD)

remaining) by 0.2 units/ml ChABC buffer (Fig. 1(*a*)). In terms of increasing incubation duration, no change in GAG quantity was apparent after 8 h of incubation. Based on these results, 0.2 units/ml ChABC buffer for 8 h was adopted as the treatment protocol. In the relatively large bovine DDFT samples, a gradient distribution of remaining GAGs was found after ChABC treatment, with 33.5 ± 17.2% left at the top of samples and ~65% remaining in the middle of samples (Fig. 1(*c*)). The contact between the container and sample surface possibly contributed to the increase of remaining GAGs to 55.4 ± 11.3% adjacent to the sample bottom. For the biomechanically tested SSTs, samples contained 48.0 ± 10.5% GAGs after ChABC treatment compared to the corresponding controls without enzyme treatment.

Based on the qualitative histological assessment, collagen density, collagen organization, and crimp of collagen fibers remained unchanged on the top and middle of samples after treatment, as evidenced by H&E-stained sections (Figs. 3(*a*)–3(*c*)). In contrast, sections from both the top and middle of treated samples showed less GAGs than corresponding sections of controls, as shown by Alcian blue stain (Figs. 3(*d*) and 3(*e*)). Consistent with the biochemical results demonstrating a gradient in GAG distribution, histological analysis showed that more GAGs were retained in the middle of treated samples (i.e., darker blue stain) than the top (Figs. 3(*e*) and 3(*f*)). Interestingly, GAG-rich pericellular matrix was observed around some fibroblasts in SST controls (Fig. 3(*g*)). ChABC treatment appeared to digest most pericellular GAGs from sections of the top and middle of the samples following enzyme incubation (Figs. 3(*h*) and 3(*i*)).

3.2 SST Mechanics After GAG Depletion. For all samples before ChABC treatment, there were no statistically significant differences detected by tendon region (i.e., anterior, posterior, medial) for peak and equilibrium stresses (Figs. 4(*a*) and 4(*b*)). All regions showed increased stresses at larger strain steps, while large differences between magnitudes of peak and equilibrium stresses clearly demonstrated that significant stress relaxation occurred. For evaluating the mechanical effect of enzyme treatment, normalized stress–relaxation curves were calculated to reduce the effect of mechanical variation of samples from different donors. ChABC treatment of samples from all three regions led to larger reductions of normalized stresses for the whole loading period compared to PBS-incubated samples (Fig. 5), demonstrating some evidence of a mechanical effect due to enzymatic GAG degradation. As no statistically significant differences in peak/equilibrium stresses or time-dependent relaxation were observed by SST region (anterior, posterior, medial), all regions were grouped together for further analysis to examine the influence of GAG depletion on tendon mechanics.

No significant differences were found for peak and equilibrium stress values computed for samples before and after ChABC treatment (Figs. 6(*a*) and 6(*b*)). Relaxation percent was also similar between samples before and after treatment, and decreased slightly at increasing strain steps (Fig. 6(*c*)). Peak and equilibrium reduced ratios were larger for samples treated by ChABC buffer than for control samples incubated in PBS, suggesting some mechanical effect of GAG degradation to tendon mechanics (i.e., larger reductions in stresses); however, these differences did not reach the level of statistical significance (Fig. 7). There was no apparent effect of strain-level on peak or equilibrium-reduced ratios for PBS-incubated or ChABC-treated samples. For microscale deformation, enzyme treatment did not alter local-matrix-based strain and rotation values (i.e., no differences when comparing samples before or after treatment); as expected, all samples exhibited increased local-matrix-based strain and rotation at greater strain levels (Fig. 8).

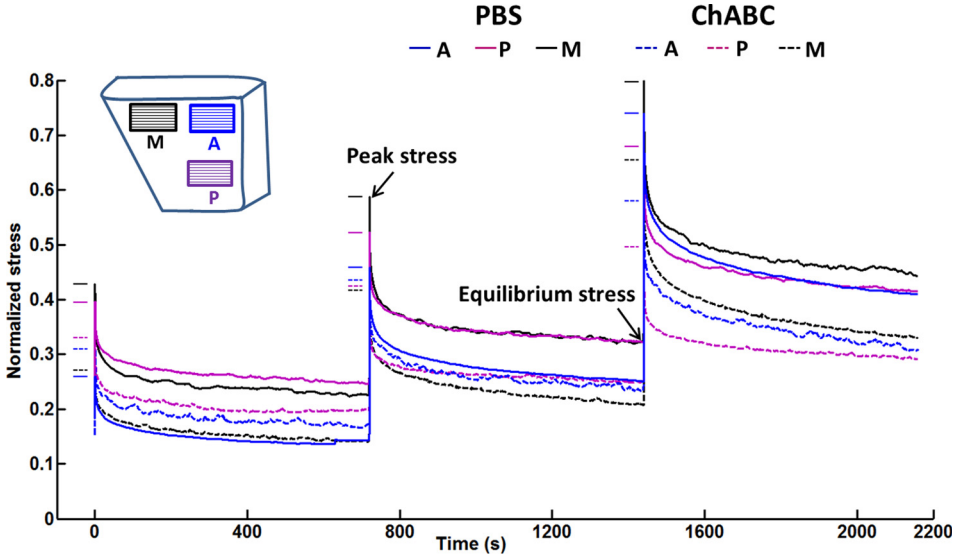

Fig. 5 Averaged stress–time curves of SST samples from anterior (A), posterior (P), and medial (M) regions after PBS incubation and ChABC treatment, normalized by corresponding peak stresses from the 0.24 strain step of mechanical test conducted before incubation or treatment. Samples subjected to ChABC treatment showed larger decreases in stress than samples following PBS incubation. Short solid and dashed lines show normalized peak stresses for each group.

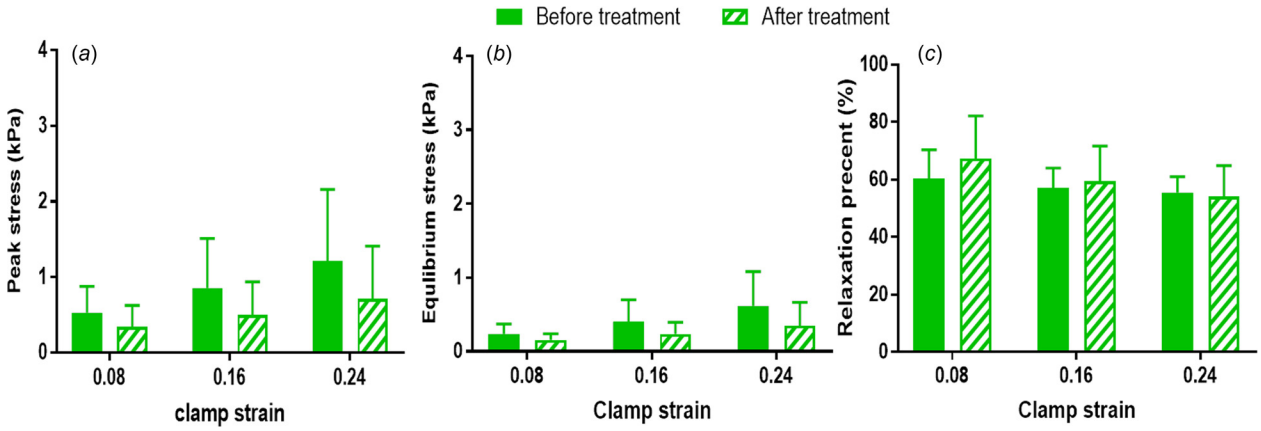

Fig. 6 Group peak stresses (*a*), equilibrium stresses (*b*), and stress relaxation percent (*c*) showed moderate changes at increasing strain steps, but were similar before and after ChABC treatment (mean ± SD)

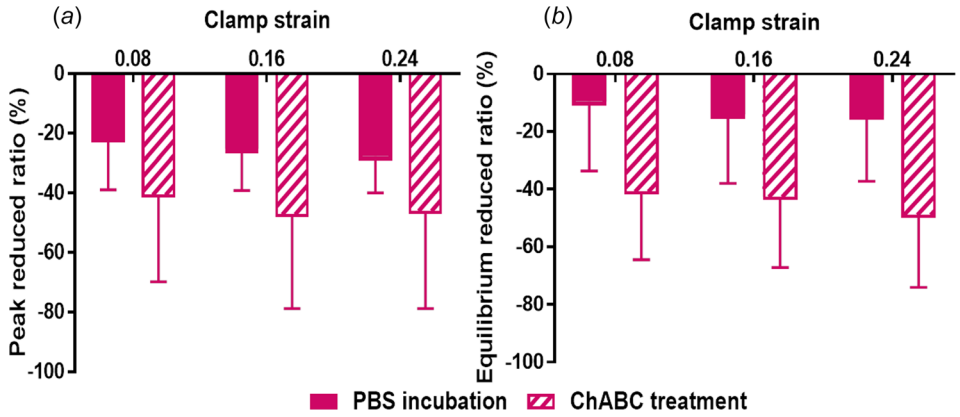

Fig. 7 Larger absolute values of peak (*a*) and equilibrium (*b*) reduced ratios after ChABC treatment compared to values following PBS incubation indicate that stresses decreased more after ChABC treatment (mean ± SD)

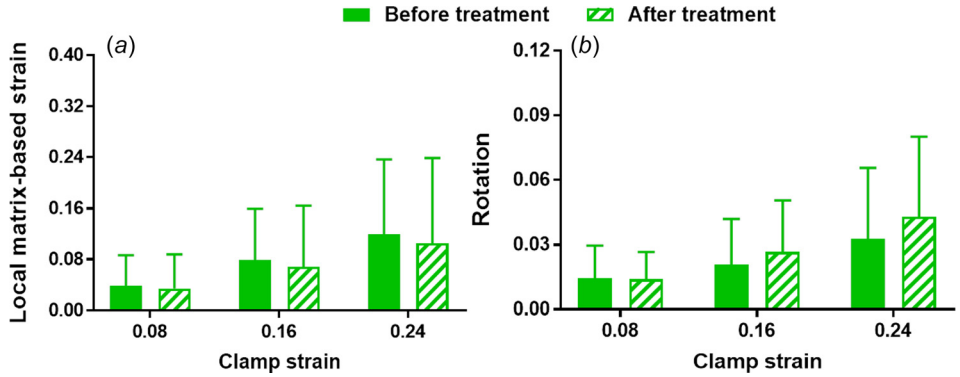

Fig. 8 Samples before and after ChABC treatment exhibit similar measures of microscale deformation, namely local-matrix-based strain (*a*) and rotation (*b*) (mean ± SD)

4 Discussion

In this study, enzymatic treatment using ChABC successfully depleted a large portion of GAGs, indicative of efficient PG degradation, from human SST prepared for shear testing. Although some of the measured values (e.g., peak/equilibrium stresses, reduced stress ratios) were decreased for enzyme-treated samples, there were no statistically significant differences between control and treated samples for any of the mechanical test results or measures of microscale deformation. These results agree with the previous reports that GAG depletion from human ligament did not change peak and equilibrium stresses at 0.25 compressive strain and tensile stress at 0.4 or 0.6 strain [12,39]. Rat tail tendons in tension also exhibited similar elastic modulus, failure stress, and failure strain before and after GAG depletion [26,27]. Given (1) the considerable heterogeneity within individual SSTs including particularly heterogeneous collagen organization and modes of deformation observed at different locations of a single SST region (Fig. 2), (2) the inherent variability across tendons from different donors including a particularly noticeable variation of GAG

amount among different SSTs, and (3) the inability to fully degrade all GAGs through enzyme treatment, it is possible that some statistically significant results would emerge if more samples were evaluated and/or if more complete GAG degradation could be achieved. Even with these considerations, the data presented in this study support the more likely conclusion that GAGs have little to no role in the mechanical behavior of SST in shear loading, and certainly do not serve as a key tissue constituent to support shear.

Previous studies [10,12,14,16,26–28,39–42] on the mechanical effect of GAGs in soft connective tissues have not always been consistent, but have been somewhat dependent on specimen species, types of soft tissues, loading modality and relative tissue health. Consistent with our findings, human medial collateral ligaments, mouse Achilles tendons, and rat tail tendons did not exhibit altered mechanical responses (i.e., stress, strain) in tension or shear after GAG removal [26–29,39,41]. Other studies showed that GAG-depleted mouse Achilles tendons had unchanged tensile stiffness, but less microscale reorganization/realignment of collagen fibers at low strains during tensile loading [23,40,42]. In contrast, injured equine superficial digital flexor tendons showed increased elastic modulus and ultimate tensile strength under tensile loading after GAG digestion [10,12,43]. Previous studies showed that GAGs likely influenced mechanical properties of soft tissues via distinct mechanisms under different loading scenarios, although it remains challenging to explicitly address the specific mechanical function of GAGs. Since highly electronegative GAGs can inhibit water exudation and further cause interstitial fluid pressurization, decreased compressive modulus of tissues such as ligament and cartilage in compression after GAG degradation are most likely attributed to the interaction between PGs and water [12,24]. For tendon, another proposed mechanism is that GAGs function as a linking structure to bridge adjacent collagen fibrils and provide load support in tension or shear [3]. Previous experimental results from different tissues, which found no change in mechanical properties after GAG digestion, cannot completely reject this suggested mechanism, but provide no supporting evidence [26,27]. One possibility is that the bond between PGs and collagen fibrils is weak or slack at low applied strain such that mechanical change due to GAG degradation in tissues is unmeasurable at many of the levels that have been evaluated experimentally [44]. Another possibility is that the influence of GAGs on tendon mechanical behavior depends on applied strain and fibril length relatively to GAG spacing, such that GAG depletion will alter tendon mechanical behavior in tension only when applied strain and the ratio of fibril length to GAG spacing are high enough [45]. A final possibility is that GAGs do not play a role in the tensile or shear mechanical response of tendon.

It is worth noting that a similar loading/analysis protocol was adopted in our prior study to investigate the mechanical role of another tissue constituent present in small quantities, namely elastin [9]. Due to similar physical constraints of the experimental setup, elastin was not fully removed after enzyme treatment; in fact, less elastin was depleted than what was achieved for GAGs in the present study [9]. Even still, SSTs were found to exhibit statistically significant decreases in stresses in shear loading after elastin degradation, particularly at low shear strains [9], similar to a study by another group [13]. Taken together, these data suggest that elastin, compared to GAGs, has a larger contribution to tendon mechanics in shear, further implying that GAGs should not be considered as a key component to regulate tendon mechanical behavior in shear.

As discussed in our prior study [9], high variability among human cadaveric SSTs due to significant natural heterogeneity and/or unknown level of age-related degeneration [9,34,35], as well as incomplete digestion of GAGs following ChABC incubation, should be considered when interpreting the current results. For example, previous studies reported higher concentrations of collagen type II, aggrecan, and biglycan in the anterior and posterior SST regions compared to the medial region, while decorin and collagen type I did not have regional variability among different regions [4,5]. Since the predominant PG in tendon is decorin, this report agrees with our result that the three different regions showed similar overall amounts of PGs and GAGs [3,5]. SST in this study also exhibited GAG-rich pericellular matrix, similar to what has been reported in cartilage, meniscus, and intervertebral disk [25]. Pericellular matrix could transduce biochemical and biomechanical signals to fibroblasts and simultaneously control/protect them by serving as viscoelastic damper [25,46]. Nonetheless, even with these potential effects, our ChABC treatment did not visibly alter SST collagen content and structure, but did reduce GAG content, including within the pericellular matrix.

To resolve the limitation of incomplete GAG depletion from tissues by ChABC treatment, genetically modified heterozygous/knockout animal models have been adopted as another approach for evaluation. Unfortunately, reports of the mechanical properties of tendons from specific PG heterozygous/knockout mice (i.e., decorin, biglycan) have been inconsistent, and appear to be influenced by tendon location, animal age, and loading protocol [14–16,47]. These discrepancies could be partially due to (1) unintended compensatory effects within tissues from these mice, including ameliorated negative influence from increased expression of other PGs in response to the down-regulation of specific targeted PGs, or (2) altered collagen fibrillogenesis due to decreased PGs during development. A combination of experimental approaches may be best suited to address the contribution of PGs and GAGs to tendon mechanics from different perspectives. As illustrated above, by examining macro- and microscale mechanical properties and deformation of ChABC treated SSTs under shear loading with two-photon microscopy, GAGs were found to minimally contribute to tendon mechanical behaviors. This study is not only consistent with several previous studies on the role of PGs and GAGs in tendon under tension [26,27,29,41], but also provides complementary knowledge of GAG function in nontensile (shear) loading.

5 Conclusion

Supraspinatus tendons showed only minor changes in mechanical and microstructural properties after ChABC treatment to remove GAGs. Heterogeneity of the relatively old donor tissues that were evaluated and incomplete digestion of GAGs may partially contribute to similarities between groups. Although these results may not fully extend to younger tendons and/or tendons following injury or repair, this study provides further evidence for a limited role of GAGs in tendon mechanics, particularly when subjected to shear loading.

Acknowledgment

This work was supported by a pilot grant from the Washington University Musculoskeletal Research Center (NIH P30 AR057235).

References

[1] September, A., Rahim, M., and Collins, M., 2016, "Towards an Understanding of the Genetics of Tendinopathy," *Metabolic Influences on Risk for Tendon Disorders*, Springer, New York, pp. 109–116.
[2] Cook, J. L., Rio, E., Purdam, C. R., and Docking, S. I., 2016, "Revisiting the Continuum Model of Tendon Pathology: What Is Its Merit in Clinical Practice and Research?," Br. J. Sports Med., **50**(19), pp. 1187–1191.
[3] Fang, F., and Lake, S. P., 2016, "Modelling Approaches for Evaluating Multiscale Tendon Mechanics," Interface Focus, **6**(1), p. 20150044.
[4] Buckley, M. R., Evans, E. B., Matuszewski, P. E., Chen, Y. L., Satchel, L. N., Elliott, D. M., Soslowsky, L. J., and Dodge, G. R., 2013, "Distributions of Types I, II and III Collagen by Region in the Human Supraspinatus Tendon," Connect. Tissue Res., **54**(6), pp. 374–379.
[5] Matuszewski, P. E., Chen, Y. L., Szczesny, S. E., Lake, S. P., Elliott, D. M., Soslowsky, L. J., and Dodge, G. R., 2012, "Regional Variation in Human Supraspinatus Tendon Proteoglycans: Decorin, Biglycan, and Aggrecan," Connect. Tissue Res., **53**(5), pp. 343–348.
[6] Fang, F., and Lake, S. P., 2015, "Multiscale Strain Analysis of Tendon Subjected to Shear and Compression Demonstrates Strain Attenuation, Fiber Sliding, and Reorganization," J. Orthop. Res., **33**(11), pp. 1704–1712.

[7] Fang, F., Sawhney, A. S., and Lake, S. P., 2014, "Different Regions of Bovine Deep Digital Flexor Tendon Exhibit Distinct Elastic, But Not Viscous, Mechanical Properties Under Both Compression and Shear Loading," J. Biomech., **47**(12), pp. 2869–2877.
[8] Stubendorff, J. J., Lammentausta, E., Struglics, A., Lindberg, L., Heinegård, D., and Dahlberg, L. E., 2012, "Is Cartilage sGAG Content Related to Early Changes in Cartilage Disease? Implications for Interpretation of dGEMRIC," Osteoarthritis Cartilage, **20**(5), pp. 396–404.
[9] Fang, F., and Lake, S. P., 2016, "Multiscale Mechanical Integrity of Human Supraspinatus Tendon in Shear After Elastin Depletion," J. Mech. Behav. Biomed. Mater., **63**, pp. 443–455.
[10] Choi, R. K., Smith, M. M., Martin, J. H., Clarke, J. L., Dart, A. J., Little, C. B., and Clarke, E. C., 2016, "Chondroitin Sulfate Glycosaminoglycans Contribute to Widespread Inferior Biomechanics in Tendon After Focal Injury," J. Biomech., **49**(13), pp. 2694–2701.
[11] Soslowsky, L. J., Thomopoulos, S., Tun, S., Flanagan, C. L., Keefer, C. C., Mastaw, J., and Carpenter, J. E., 2000, "Neer Award 1999: Overuse Activity Injures the Supraspinatus Tendon in an Animal Model: A Histologic and Biomechanical Study," J. Shoulder Elbow Surg., **9**(2), pp. 79–84.
[12] Henninger, H. B., Underwood, C. J., Ateshian, G. A., and Weiss, J. A., 2010, "Effect of Sulfated Glycosaminoglycan Digestion on the Transverse Permeability of Medial Collateral Ligament," J. Biomech., **43**(13), pp. 2567–2573.
[13] Grant, T. M., Yapp, C., Chen, Q., Czernuszka, J. T., and Thompson, M. S., 2015, "The Mechanical, Structural, and Compositional Changes of Tendon Exposed to Elastase," Ann. Biomed. Eng., **43**(10), pp. 2477–2486.
[14] Dunkman, A. A., Buckley, M. R., Mienaltowski, M. J., Adams, S. M., Thomas, S. J., Kumar, A., Beason, D. P., Iozzo, R. V., Birk, D. E., and Soslowsky, L. J., 2014, "The Injury Response of Aged Tendons in the Absence of Biglycan and Decorin," Matrix Biol., **35**, pp. 232–238.
[15] Dourte, L. M., Pathmanathan, L., Mienaltowski, M. J., Jawad, A. F., Birk, D. E., and Soslowsky, L. J., 2013, "Mechanical, Compositional, and Structural Properties of the Mouse Patellar Tendon With Changes in Biglycan Gene Expression," J. Orthop. Res., **31**(9), pp. 1430–1437.
[16] Dourte, L. M., Pathmanathan, L., Jawad, A. F., Iozzo, R. V., Mienaltowski, M. J., Birk, D. E., and Soslowsky, L. J., 2012, "Influence of Decorin on the Mechanical, Compositional, and Structural Properties of the Mouse Patellar Tendon," ASME J. Biomech. Eng., **134**(3), p. 031005.
[17] Fang, F., and Lake, S. P., 2017, "Experimental Evaluation of Multiscale Tendon Mechanics," J. Orthop. Res., epub.
[18] Iozzo, R. V., 1997, "The Family of the Small Leucine-Rich Proteoglycans: Key Regulators of Matrix Assembly and Cellular Growth," Crit. Rev. Biochem. Mol. Biol., **32**(2), pp. 141–174.
[19] Landis, W. J., and Silver, F. H., 2002, "The Structure and Function of Normally Mineralizing Avian Tendons," Comp. Biochem. Physiol., Part A: Mol. Integr. Physiol., **133**(4), pp. 1135–1157.
[20] Robbins, J. R., Evanko, S. P., and Vogel, K. G., 1997, "Mechanical Loading and TGF-β Regulate Proteoglycan Synthesis in Tendon," Arch. Biochem. Biophys., **342**(2), pp. 203–211.
[21] Feitosa, V. L. C., Reis, F. P., Esquisatto, M. A. M., Joazeiro, P. P., Vidal, B. C., and Pimentel, E. R., 2006, "Comparative Ultrastructural Analysis of Different Regions of Two Digital Flexor Tendons of Pigs," Micron, **37**(6), pp. 518–525.
[22] Nissi, M. J., Salo, E. N., Tiitu, V., Liimatainen, T., Michaeli, S., Mangia, S., Ellermann, J., and Nieminen, M. T., 2015, "Multi-Parametric MRI Characterization of Enzymatically Degraded Articular Cartilage," J. Orthop. Res., **34**(7), pp. 1111–1120.
[23] Schmidt, M. B., Mow, V. C., Chun, L. E., and Eyre, D. R., 1990, "Effects of Proteoglycan Extraction on the Tensile Behavior of Articular Cartilage," J. Orthop. Res., **8**(3), pp. 353–363.
[24] Soltz, M. A., and Ateshian, G. A., 2000, "Interstitial Fluid Pressurization During Confined Compression Cyclical Loading of Articular Cartilage," Ann. Biomed. Eng., **28**(2), pp. 150–159.
[25] Wilusz, R. E., Sanchez-Adams, J., and Guilak, F., 2014, "The Structure and Function of the Pericellular Matrix of Articular Cartilage," Matrix Biol., **39**, pp. 25–32.
[26] Fessel, G., and Snedeker, J. G., 2009, "Evidence Against Proteoglycan Mediated Collagen Fibril Load Transmission and Dynamic Viscoelasticity in Tendon," Matrix Biol., **28**(8), pp. 503–510.
[27] Fessel, G., and Snedeker, J. G., 2011, "Equivalent Stiffness After Glycosaminoglycan Depletion in Tendon—An Ultra-Structural Finite Element Model and Corresponding Experiments," J. Theor. Biol., **268**(1), pp. 77–83.
[28] Lujan, T. J., Underwood, C. J., Henninger, H. B., Thompson, B. M., and Weiss, J. A., 2007, "Effect of Dermatan Sulfate Glycosaminoglycans on the Quasi-Static Material Properties of the Human Medial Collateral Ligament," J. Orthop. Res., **25**(7), pp. 894–903.
[29] Svensson, R. B., Hassenkam, T., Hansen, P., Kjaer, M., and Magnusson, S. P., 2011, "Tensile Force Transmission in Human Patellar Tendon Fascicles Is Not Mediated by Glycosaminoglycans," Connect. Tissue Res., **52**(5), pp. 415–421.
[30] Gandley, R. E., McLaughlin, M. K., Koob, T. J., Little, S. A., and McGuffee, L. J., 1997, "Contribution of Chondroitin-Dermatan Sulfate-Containing Proteoglycans to the Function of Rat Mesenteric Arteries," Am. J. Physiol.: Heart Circ. Physiol., **273**(2), pp. H952–H960.
[31] Mattson, J. M., Turcotte, R., and Zhang, Y., 2016, "Glycosaminoglycans Contribute to Extracellular Matrix Fiber Recruitment and Arterial Wall Mechanics," Biomech. Model. Mechanobiol., **4**, pp. 1–13.
[32] Deprés-Tremblay, G., Chevrier, A., Snow, M., Hurtig, M. B., Rodeo, S., and Buschmann, M. D., 2016, "Rotator Cuff Repair: A Review of Surgical Techniques, Animal Models, and New Technologies Under Development," J. Shoulder Elbow Surg., **25**(12), pp. 2078–2085.
[33] Bey, M. J., Ramsey, M. L., and Soslowsky, L. J., 2002, "Intratendinous Strain Fields of the Supraspinatus Tendon: Effect of a Surgically Created Articular-Surface Rotator Cuff Tear," J. Shoulder Elbow Surg., **11**(6), pp. 562–569.
[34] Lake, S. P., Miller, K. S., Elliott, D. M., and Soslowsky, L. J., 2009, "Effect of Fiber Distribution and Realignment on the Nonlinear and Inhomogeneous Mechanical Properties of Human Supraspinatus Tendon Under Longitudinal Tensile Loading," J. Orthop. Res., **27**(12), pp. 1596–1602.
[35] Lake, S. P., Miller, K. S., Elliott, D. M., and Soslowsky, L. J., 2010, "Tensile Properties and Fiber Alignment of Human Supraspinatus Tendon in the Transverse Direction Demonstrate Inhomogeneity, Nonlinearity, and Regional Isotropy," J. Biomech., **43**(4), pp. 727–732.
[36] Zheng, C., and Levenston, M. E., 2015, "Fact Versus Artifact: Avoiding Erroneous Estimates of Sulfated Glycosaminoglycan Content Using the Dimethylmethylene Blue Colorimetric Assay for Tissue-Engineered Constructs," Eur. Cells Mater., **29**, pp. 224–236.
[37] Koob, T. J., and Vogel, K. G., 1987, "Site-Related Variations in Glycosaminoglycan Content and Swelling Properties of Bovine Flexor Tendon," J. Orthop. Res., **5**(3), pp. 414–424.
[38] Grant, T. M., Thompson, M. S., Urban, J., and Yu, J., 2013, "Elastic Fibres Are Broadly Distributed in Tendon and Highly Localized Around Tenocytes," J. Anat., **222**(6), pp. 573–579.
[39] Lujan, T. J., Underwood, C. J., Jacobs, N. T., and Weiss, J. A., 2009, "Contribution of Glycosaminoglycans to Viscoelastic Tensile Behavior of Human Ligament," J. Appl. Physiol., **106**(2), pp. 423–431.
[40] Millesi, H., Reihsner, R., Hamilton, G., Mallinger, R., and Menzel, E. J., 1995, "Biomechanical Properties of Normal Tendons, Normal Palmar Aponeuroses, and Tissues From Patients With Dupuytren's Disease Subjected to Elastase and Chondroitinase Treatment," Clin. Biomech., **10**(1), pp. 29–35.
[41] Rigozzi, S., Müller, R., and Snedeker, J. G., 2009, "Local Strain Measurement Reveals a Varied Regional Dependence of Tensile Tendon Mechanics on Glycosaminoglycan Content," J. Biomech., **42**(10), pp. 1547–1552.
[42] Rigozzi, S., Müller, R., Stemmer, A., and Snedeker, J. G., 2013, "Tendon Glycosaminoglycan Proteoglycan Sidechains Promote Collagen Fibril Sliding—AFM Observations at the Nanoscale," J. Biomech., **46**(4), pp. 813–818.
[43] Isaacs, J. L., Vresilovic, E., Sarkar, S., and Marcolongo, M., 2014, "Role of Biomolecules on Annulus Fibrosus Micromechanics: Effect of Enzymatic Digestion on Elastic and Failure Properties," J. Mech. Behav. Biomed. Mater., **40**, pp. 75–84.
[44] Watanabe, T., Kametani, K., Koyama, Y., Suzuki, D., Imamura, Y., Takehana, K., and Hiramatsu, K., 2016, "Ring-Mesh Model of Proteoglycan Glycosaminoglycan Chains in Tendon Based on Three-Dimensional Reconstruction by Focused Ion Beam Scanning Electron Microscopy," J. Biol. Chem., **291**(45), pp. 23704–23708.
[45] Ahmadzadeh, H., Connizzo, B. K., Freedman, B. R., Soslowsky, L. J., and Shenoy, V. B., 2013, "Determining the Contribution of Glycosaminoglycans to Tendon Mechanical Properties With a Modified Shear-Lag Model," J. Biomech., **46**(14), pp. 2497–2503.
[46] Han, W. M., Heo, S. J., Driscoll, T. P., Delucca, J. F., McLeod, C. M., Smith, L. J., Duncan, R. L., Mauck, R. L., and Elliott, D. M., 2016, "Microstructural Heterogeneity Directs Micromechanics and Mechanobiology in Native and Engineered Fibrocartilage," Nat. Mater., **15**(4), pp. 477–484.
[47] Gordon, J. A., Freedman, B. R., Zuskov, A., Iozzo, R. V., Birk, D. E., and Soslowsky, L. J., 2015, "Achilles Tendons From Decorin-and Biglycan-Null Mouse Models Have Inferior Mechanical and Structural Properties Predicted by an Image-Based Empirical Damage Model," J. Biomech., **48**(10), pp. 2110–2115.